Effectiveness of UN-GdN Burnable Absorber for 180MWt SMR Core loaded with LEU+ Fuels

Seung Taek Oh and Ser Gi Hong*
Department of Nuclear Engineering Hanyang University
firebearos12@hanyang.ac.kr; *Corresponding author: hongsergi@hanyang.ac.kr

Keywords : SMRs, LEU+, UN-GdN

1. Introduction

The increasing electricity demand from AI and data centers has emerged as a critical global challenge. In response, Small Modular Reactors (SMRs) are being investigated as a potential solution due to their flexible installation and lower initial investment costs. However, the small core size inherently increases neutron leakage, which reduces cycle length and discharge burnup. To mitigate these issues, Low Enriched Uranium Plus (LEU+) fuel, enriched between 5–10 wt. %, is introduced to extend cycle lengths and to enhance discharge burnup.

However, adoption of LEU+ fuel may require more burnable absorbers (BA) to suppress higher excess reactivity throughout the cycle. Nevertheless, increasing gadolinia content in conventional UO_2-Gd_2O_3 BA rods is not straightforward, since thermal conductivity deteriorates with higher gadolinia weight percent [1].

To overcome these limitations, this study proposes a hybrid core design concept that employs a new BA, UN-GdN, while retaining standard UO_2 for the remaining fuel rods. This configuration is primarily driven by the superior properties of the nitride system; UN possesses a higher density than UO_2 and GdN contains approximately 31% more gadolinium atoms per unit volume than Gd_2O_3, providing higher neutron absorption capability [2]. Furthermore, the UN-GdN itself exhibits superior thermal conductivity compared to conventional UO_2-Gd_2O_3 [1][2].

To support the extended cycle length and ensure fuel rod integrity under the higher enrichment conditions, the Accident-Tolerant Fuel (ATF) concept, specifically chromium (Cr)-coated cladding, is integrated into the design. By utilizing this hybrid approach, this study evaluates the anticipated benefits of achieving an extended cycle length and higher discharge burnup in a 180 MWt SMR comprised of 37 fuel assemblies.

2. Design and Methodologies

2.1 Fuel and Burnable Absorber Rods Design

Table I summarizes the design specifications of the fuel and UN-GdN BA rods. The fuel rods consist of UO_2 with an enrichment of 5.0-7.0 wt. %, while the UN-GdN BA rods were configured with a GdN content of 6.0 ~ 15.0 wt. % and a reduced uranium enrichment of 3 wt. % to suppress initial excess reactivity and to mitigate local power peaking.

The fuel rods and BA rods were designed with identical geometric dimensions. The pellet radii for both are 0.4096 cm. The cladding is composed of Zircaloy-4 where inner and outer radii are 0.4178 and 0.4750 cm respectively. Furthermore, a Chromium (Cr) coating with a thickness of 15 μm was applied to the outer surface of the cladding to inhibit high-temperature oxidation and ensure structural integrity. The detailed configurations are shown in **Fig 1.**

Table I. Specification of UN-GdN BA and fuel rod

UN-GdN BA rod	
UN enrichment (wt. %)	3.0
Fraction of GdN (wt. %)	6.0 ~ 15.0
UN density (g/cm^3)	14.2
GdN density (g/cm^3)	9.11
pellet radius (cm)	0.4096
Cladding inner / outer radius (cm)	0.4178 / 0.4750
Cr coating thickness (μm)	15
UO_2 fuel rod	
U-235 enrichment (wt. %)	5.0 ~ 7.0
Fuel pellet density (g/cm^3)	10.220
pellet radius (cm)	0.4096
Cladding inner / outer radius (cm)	0.4178 / 0.4750
Cr coating thickness (μm)	15

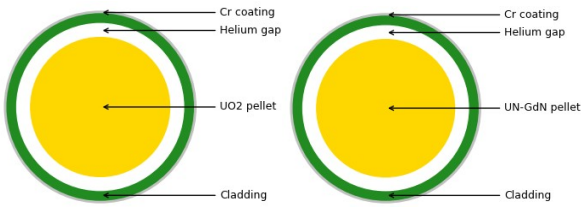

Fig. 1. Radial Configuration of Fuel and BA Rods

2.2 Fuel Assembly and Core Design

The core utilizes a Westinghouse 17 x 17 type fuel assembly (FA) with a total thermal power of 180MW_{th}. To enhance discharge burnup, a 3-batch refueling strategy was adopted. Stainless steel 304 (SS304) was

also employed as the reflector material to minimize neutron leakage and improve neutron economy. To ensure the operational safety and performance of the core, several design targets were applied. These targets include the F_q, F_r and Axial offset (AO). **Table II** shows the design parameters of the core.

Table II. Core design parameters

Core	
Core thermal power (MW_{th})	180
Number of FAs	37
Fuel management scheme	3 batch
Radial reflector	Stainless steel 304
Fuel assembly	
Fuel rod array square	17 x 17
FA pitch (cm)	21.5
Fuel pin pitch (cm)	1.26
Number of instrument / guide tubes	24 / 1
Number of fuel rod	264
Design target constraints	
Axial offset	-0.3 < AO < 0.3
Maximum F_q	2.8
Maximum F_r	1.7

2.3 Computer Codes

For the neutronic analysis, a two-step calculation procedure is adopted by the DeCART2D [3] and MASTER [4] (developed by KAERI). In the first step, DeCART2D solves the 2D neutron transport equation using the Method of Characteristics. Based on an ENDF/B VII.1 nuclear data library, DeCART2D employs a 47-group neutron and 18-group gamma structure to generate FA-wise homogenized group constants (HGC) for subsequent core calculations.

In the second step, the homogenized two-group constants from DeCART2D are utilized to MASTER, which performs 3D full-core nodal diffusion calculations. MASTER uses the Source Expansion Nodal Method, supporting both steady-state and transient simulation.

3. Design Analysis and Results

3.1 Assembly-level Analysis

In conventional core designs, multiple FA types with different BA-rod loadings are typically employed to control excess reactivity and the power distribution.

In contrast, this study adopts a single, uniform FA design in which every FA incorporates exactly 32 UN-GdN burnable absorber rods. As shown in **Fig. 2**, the 32 BA rods are appropriately arranged around the guide tubes. **Fig. 3** shows the infinite multiplication factor (k_{inf}) for designed FAs. The calculated k_{inf} shows stable behavior over burnup, indicating that the specific enrichment levels successfully balance the fuel depletion of the LEU+ fuel.

This stable reactivity behavior suggests that the design requirements are met with a simplified FA design configuration, effectively avoiding the complexity of using numerous assembly types. The specifications of the designed fuel assemblies are summarized in **Table III**.

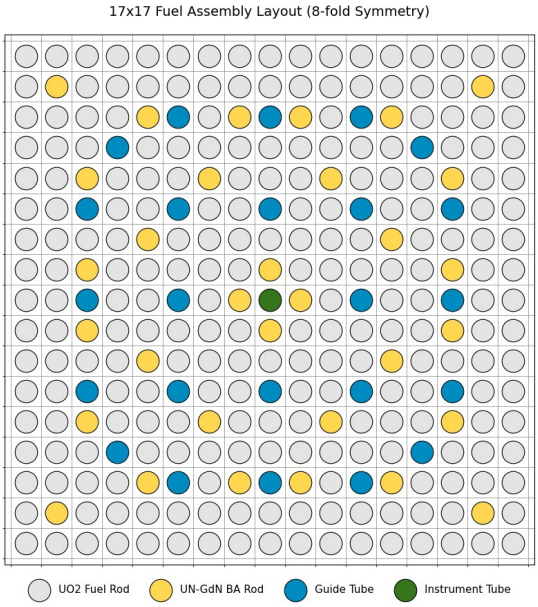

Fig. 2 Radial configuration of FA with 32 BA Rods

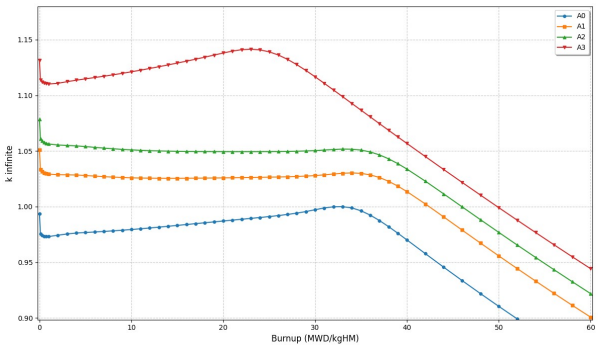

Fig. 3 Comparison of k_{inf} with respect to FAs

Table III. Detailed Enrichment and GdN Loading Specifications for Each FA Type

Type	**A0**	**A1**	**A2**	**A3**
U enrichment (wt. %) in UO_2	5	6	6.5	7
U enrichment (wt. %) in UN-GdN	3	3	3	3
GdN (wt. %) in UN-GdN	13	12	11	6
Total number of BA rods in FA	32	32	32	32

3.2 Core Design and Loading Strategy

To maximize the discharge burnup and enhance fuel utilization, a 3-batch refueling strategy was implemented for the core design. Unlike conventional strategies where the central FA might be replaced more frequently, this study employs a specific loading pattern. Specifically, the refueling scheme follows a sequence of replacing 13 FAs, 12 FAs, and 12 FAs in a rotating sequence, where the central FA (A1) is replaced only once every three cycles to maximize its discharge burnup. Meanwhile, the remaining 12 fresh FAs in each reloading batch are replaced with A3 type FAs.

3.2.1 Analysis of Cycles 1 to *6*

The detailed core configurations for Cycles 1 to 3 are illustrated in **Fig. 4** and **Fig. 5**. A key characteristic of the initial core is the utilization of A0 FAs, which are exclusively employed in Cycle 1 to establish the baseline core reactivity.

As shown in **Table IV**, the first cycle achieved a cycle length of 1358.38 EFPD with a remarkably low critical boron concentration (CBC) of 288.22 ppm. For the second cycle, to compensate for reactivity depletion, the central A0 FA was replaced with an A1 FA, along with other strategic reloads, totaling 13 assembly replacements. This transition resulted in a cycle length of 951.70 EFPD.

After the second cycle, the refueling scheme follows a sequence of replacing 13 FAs, 12 FAs, and 12 FAs in a rotating sequence. From the third cycle onward, cycle lengths ranged from 900.00 to 1009.57 EFPD. The maximum boron concentrations remained below 1148 ppm across all cycles. Throughout these operations, the core performance consistently satisfied all design constraints, including F_r, F_q and axial offset (AO). The detailed performance metrics for Cycles 1 to 6 are illustrated in **Fig. 6**, **Fig. 7**, and **Fig. 8**.

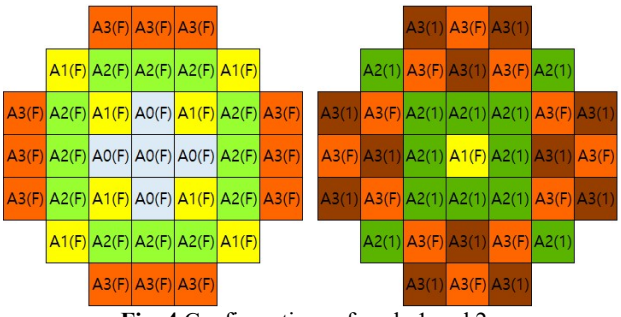

Fig. 4 Configurations of cycle 1 and 2

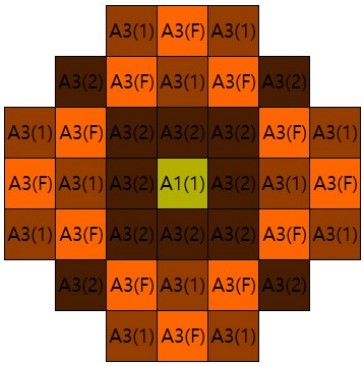

Fig. 5 Configurations of cycle 3

Table IV. Result of the first cycle

Cycle		1
EFPD		1358.38
Maximum CBC (ppm)		288.22
Maximum F_r		1.5133
Maximum F_q		2.1857
Maximum axial offset in absolute value		0.1188
MTC (pcm/°C)	HFP (BOC / EOC)	-55.45 / -69.38
	HZP (BOC / EOC)	-37.50 / -47.88

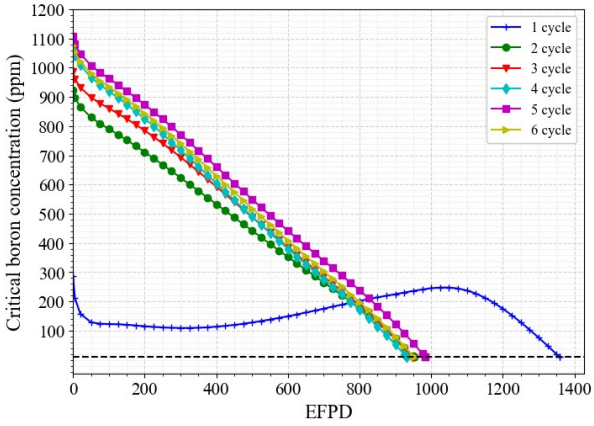

Fig. 6 Evolution of CBC with respect to EFPD for cycle 1 ~ 6

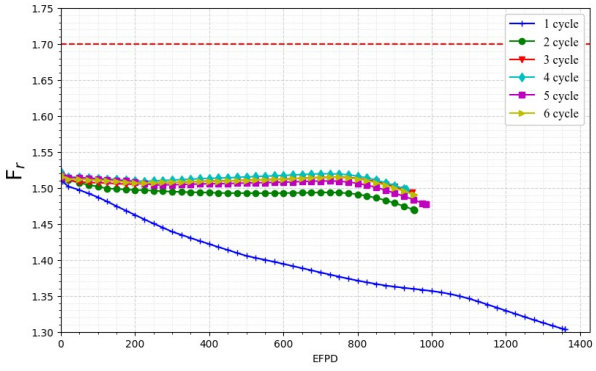

Fig. 7 Evolution of F_r with respect to EFPD for cycle 1 ~ 6

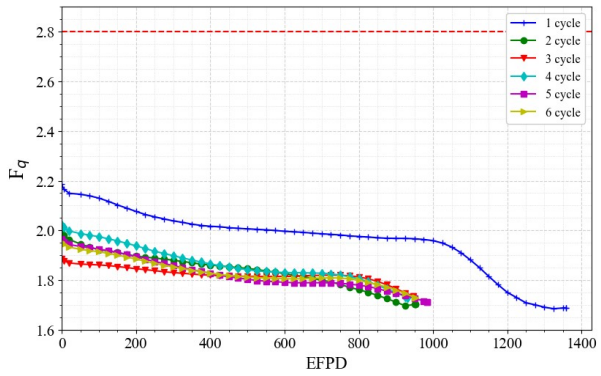

Fig. 8 Evolution of F_q with respect to EFPD for cycle 1-6

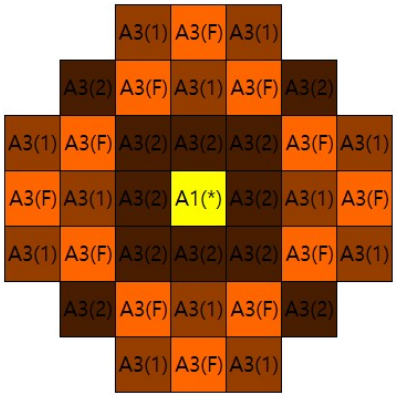

Fig. 9 Configuration of Equilibrium cycles

3.2.2 Analysis of equilibrium cycles

The detailed core configurations for Equilibrium cycles are illustrated in **Fig. 9**. The core reaches equilibrium state roughly at the 14th cycle. Due to the replacement of the central A1 assembly every 2 + 3n cycles, the equilibrium state consists of three distinct cycle types as summarized in **Table V**. These equilibrium cycles achieved lengths of 991.62, 947.14, and 925.32 EFPD, respectively. The maximum CBC during equilibrium cycles ranged from 1032 to 1120 ppm. The moderator temperature coefficient (MTC) remained negative under all conditions. As shown in **Table VI**, the discharge burnup of A1, the FA located in the core center, was calculated to be 56.85 MWD/kgHM. While the A3 FA, where 12 assemblies are replaced per cycle, exhibited a lower discharge burnup of 53.65 MWD/kgHM.

Consequently, the average discharge burnup for the entire core was determined to be 53.73 MWD/kgHM. Also, safety criteria were strictly met across all cycles, including both the transient and equilibrium stages, ensuring the operational safety of the proposed SMR core.

Table V. Result of the Equilibrium cycles core parameters

Equilibrium cycle		Type 1	Type 2	Type 3
EFPD		991.62	947.14	925.32
Maximum CBC (ppm)		1119.55	1073.05	1032.63
Maximum F_r		1.5137	1.5222	1.5262
Maximum F_q		1.9606	1.9620	1.9682
Maximum AO in absolute value		0.0322	0.0332	0.0395
MTC (pcm/°C)	HFP (BOC / EOC)	-41.47 / -75.11	-42.44 / -75.38	-43.39/ -75.80
	HZP (BOC / EOC)	-25.06 / -52.61	-25.82 / -52.72	-26.68/ -52.94

Table VI. Average FA Discharge Burnup in the Equilibrium Cycles Core

FA types	A1	A3
Average FA burnup (MWD/kgHM)	56.85	53.65
Core average discharge burnup (MWD/kgHM)	53.73	

4. CONCLUSION

This study proposed a preliminary core design for a 180 MWt Small Modular Reactor (SMR) utilizing LEU+ fuel (5-7 wt. % UO_2) and Uranium Nitride-Gadolinium Nitride (UN-GdN) burnable absorber (BA) rods. The analysis confirmed that a configuration using 32 UN-GdN BA rods per assembly, with varying GdN contents of 6, 11, 12, and 13 wt. % integrated into a 3% enriched UN matrix, effectively stabilizes the high excess reactivity of LEU+ fuel. The entire core operation can be sustained using only 4 standardized FA types. The 3D full-core analysis conducted with the MASTER code revealed that all essential safety parameters, including F_r, F_q, and Axial Offset, strictly adhered to the design limits across both the initial and equilibrium cycles under a 3-batch refueling strategy. Specifically, the initial cycle achieved 1358.38 EFPD while maintaining CBC of only 287.54 ppm. In the equilibrium cycles, the core cycle lengths were 991.62, 947.14, and 925.32 EFPD respectively, ensuring that the CBC remained below 1120 ppm. The average discharge burnup at equilibrium cycles is 53.73 MWD/kgHM.

While these results prove the feasibility of the heterogeneous core configuration with UN-GdN BA rods, this preliminary design will serve as a baseline for future studies. Subsequent research will employ meta-heuristic optimization techniques, such as Simulated Annealing (SA), to further explore the vast combinatorial space of fuel and BA placements, aiming to maximize cycle length and thermal safety margins.

5. Acknowledgment

This work was supported by the Korea Institute of Energy Technology Evaluation and Planning (KETEP) and the Ministry of Climate, Energy & Environment (MCEE) of the Republic of Korea (No. RS-2024-00398867).

REFERENCES

[1] HIRAI, M., & ISHIMOTO, S. (1991). Thermal Diffusivities and Thermal Conductivities of UO_2-Gd_2O_3 . *Journal of Nuclear Science and Technology*, *28*(11), 995–1000. https://doi.org/10.1080/18811248.1991.9731462
[2] Kim, Gyeonghun & Ahn, Sangjoon. (2021). Thermal conductivity of gadolinium added uranium mononitride fuel pellets sintered by spark plasma sintering. Journal of Nuclear Materials. 546. 152785. 10.1016/j.jnucmat.2021.152785.
[3] J. Y. Cho et al., "DeCART2D v1.0 User's Manual, KAERI/TR-5116/2013.
[4] J. Y. Cho et al., "MASTER 3.0 User's Manual", KAERI/UM-8/2004.